

Implementation of a micro ball lens on a silicon optical bench using insoluble two-phase liquid immersion technology

Chih-Chun Lee¹, Sheng-Yi Hsiao² and Weileun Fang^{1,2,3}

¹ Institute of NanoEngineering and MicroSystems, Hsinchu, 30013, Taiwan, Republic of China

² Power Mechanical Engineering, National Tsing Hua University, Hsinchu, 30013, Taiwan, Republic of China

E-mail: fang@pme.nthu.edu.tw

Received 17 March 2010, in final form 29 May 2010

Published 8 July 2010

Online at stacks.iop.org/JMM/20/085015

Abstract

This paper presents a two-phase liquid micro lens formation technology to implement a polymer micro ball lens. A UV-curable polymer is dispensed into a buffer liquid to form the ball lens. The buffer liquid provides a gravity-free condition so that the ball lens has a highly symmetric shape. The diameter of the ball lens is controlled by the volume of the dispensed polymer. This technology implements either a discrete optical component, or a ball lens integrated with a MEMS (micro electrical mechanical system) structure to form a SiOB (silicon optical bench). To demonstrate the feasibility of this study, ball lenses with diameters ranging from 200 to 600 μm and root mean square (RMS) surface roughness of about 10 nm are fabricated using a commercial UV-curable polymer. The average roundness of a 550 μm diameter ball lens observed from different angles is $3.3 \pm 0.4 \mu\text{m}$. The peak-to-valley and RMS wavefront errors of a 550 μm diameter ball lens measured by a Mach-Zehnder interferometer are 0.3744 waves (237 nm) and 0.0766 waves (48 nm), respectively. The measured back focal length is about 99 μm , and the associated effective focal length is about 351 μm . The integration of such polymer micro ball lenses with suspended micromachined Si_3N_4 structures to form the SiOB is also demonstrated.

(Some figures in this article are in colour only in the electronic version)

1. Introduction

Presently, the miniaturization and integration of micro optical components are of interest in many applications. Thus, a MEMS (micro electrical mechanical systems)-based silicon optical bench (SiOB) has been widely studied [1]. A three-dimensional (3D) micro ball lens is a key component for the SiOB. For instance, the ball lens is used in optical fiber probes for biomedical spectroscopy [2], add-drop multiplexers [3], optical encoder systems [4], optical resonators [5], etc. A discrete micro ball lens with diameter D larger than 300 μm is commercially available. However, it is not simple to integrate such discrete micro ball lenses with the SiOB by means of assembly. On the other hand, the micro lens can be

fabricated and integrated on the SiOB using microfabrication technologies. For example, etching selectivity techniques have been exploited to form a silicon micro lens [6]. The photoresist reflow process commonly applied to micro lens manufacturing has been reported in [7–9]. As discussed in [8], LIGA technology is used to define the resist shape (usually PMMA) with deep x-rays and then applying the thermal reflow process to form the micro lens. Compared with the reflow process techniques, a nozzle is employed in [10] to dispense the liquid polymer droplet onto a substrate.

The aforementioned fabricating technologies mainly implement the micro lenses with their optical axes along the out-of-plane direction. Such micro lenses are more appropriate for the SiOB with the light beam incident in the out-of-plane direction. However, it is difficult to exploit these micro lenses on the SiOB formed by in-plane optical components.

³ Author to whom any correspondence should be addressed.

In this regard, various microfabrication processes have been presented to realize the micro lens for the in-plane SiOB [11]. In addition, the approaches to lift up and assemble the micro optical components have also been exploited to implement the in-plane SiOB [12]. In order to realize the components' assembly, relatively complicated structures and fabrication processes are required. Therefore, it is challenging to improve the accuracy and yield for these approaches.

This study reports a new approach to fabricate discrete micro ball lenses under gravity-free and non-wetting liquid ambient conditions. The liquid-phase polymer, which is suspended and insoluble in the liquid medium, will form a sphere caused by the surface tension. After that, the polymer is solidified inside the liquid medium by using UV light to define the lens shape [13]. The liquid-phase-formed lens is of high surface quality. Moreover, the lens diameter can easily be controlled by simply changing the volume of the liquid polymer. The formation of such polymer ball lenses can also be achieved on a Si substrate with suspended micromachined structures. Thus, the ball lens can further integrate with the Si substrate and suspended micromachined structures without the assembly process. Such ball lenses are easily employed for the SiOB with optical axes in the in-plane as well as out-of-plane directions.

2. Concept and process design

The existing liquid-phase-formed polymer micro lens has been successfully implemented on various solid supporting structures, for instance, silicon, glass or quartz substrates [14], micromachined thin film structures [12], etc. The formation of such polymer lenses takes place under air ambient conditions. In this regard, the final shape of a lens is determined by the static equilibrium of the following three forces: surface tension, gravity and reaction forces from supporting structures. Thus, the lens curvature is mainly determined by the volume and surface tension of the polymer. According to the gravitational and reaction forces from the supporting structure, the microlens is plano-convex or biconvex [12, 14]. To minimize the influence of forces other than surface tension, this study presents the concept of forming the micro polymer ball lens under liquid ambient conditions (named two-phase liquid microlens formation technology). As shown in figure 1(a), the liquid-phase polymer (UV-curable) is dispensed into the immiscible buffer liquid, and thus, the polymer droplet is subjected to both gravity and buoyancy. UV light is then employed to solidify the polymer, as shown in figure 1(b). In order to achieve the formation of a ball lens, the density of the buffer liquid is selected to be approximately the same as that of the dispensed polymer. Thus, the gravity and buoyancy applied to the polymer droplet are balanced, and the surface tension becomes the only force remaining on the droplet as shown in figure 2. As a result, the surface area of the droplet is minimized by the surface tension. The droplet is then shaped into a perfect sphere that has the smallest surface area to volume ratio. This approach enables the fabrication of the discrete micro polymer ball lens. Moreover, the diameter

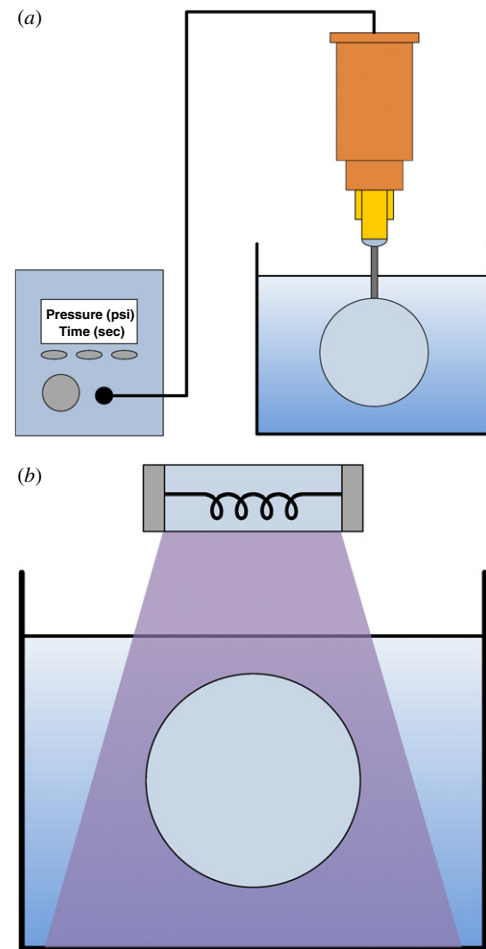


Figure 1. The concept of the presented approach, the liquid-phase polymer is (a) dispensed into the immiscible buffer liquid, and then (b) solidified by UV light.

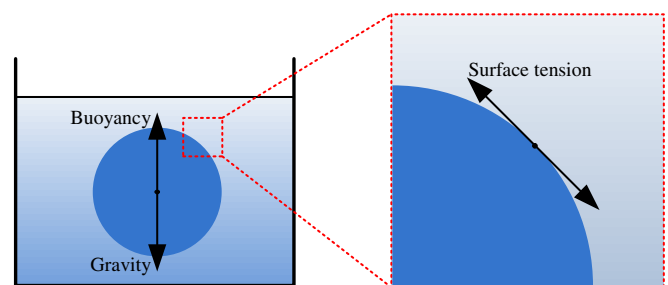


Figure 2. Polymer droplet in the liquid medium is gravity-free. A spherical ball lens is formed to satisfy the minimum energy.

of the micro ball lens can be determined by the volume of the dispensed polymer.

Figure 3 further shows the concept of formation and integration of the micro ball lens with other micromachined components. As shown in figures 3(a) and (b), the Si substrate was etched using DRIE and then silicon nitride was deposited and patterned. As shown in figure 3(c), the silicon nitride was suspended to form the lens frame (single-side and double-side) after the Si substrate underneath was removed using the KOH solution. The U-shape cross section of the nitride film defined by the trench in figure 3(a) is employed to increase the stiffness of the lens frame [15]. The Si substrate containing

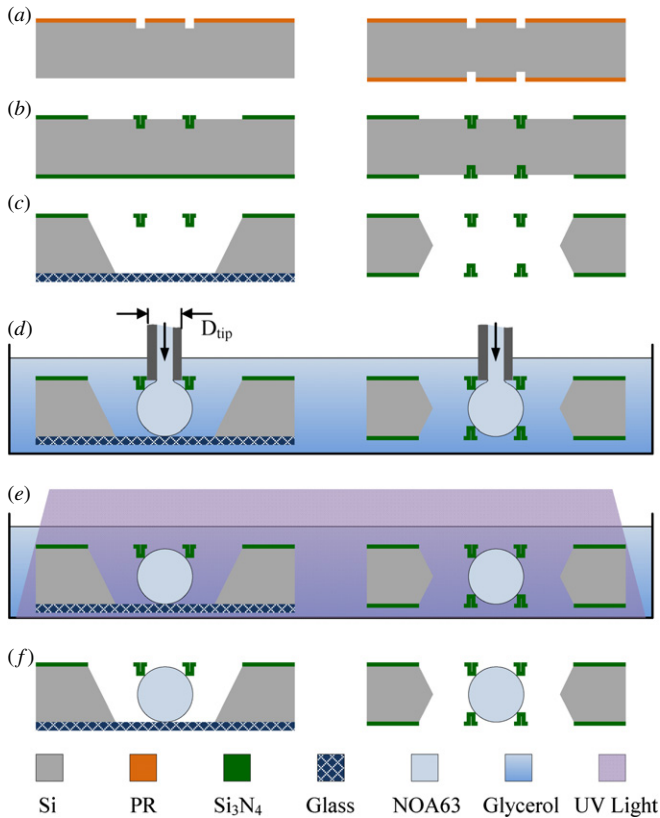


Figure 3. Formation and integration of the ball lens with a MEMS structure for SiOB.

the single-side lens frame can be further bonded with a Pyrex glass. As shown in the device on the left-hand side of figure 3(d), the Si substrate with the suspended lens frame is immersed into a buffer liquid. The UV-curable polymer droplet is then dispensed between the micromachined frame and Pyrex glass. After that, the polymer is solidified by means of UV curing in the buffer liquid as shown in figure 3(e). Finally, the solid polymer ball lens is formed, and is also simultaneously assembled on the Si substrate consisting of the micromachined frame and Pyrex glass, as shown in the device on the left-hand side of figure 3(f). The solid ball lens is thus confined by the suspended micromachined frame and Pyrex glass. By using the same process, the micro ball lens can also be simultaneously fabricated and integrated on various SiOBs consisting of different micromachined components. For instance, as indicated in the device on the right-hand side of figures 3(d)–(f), the cured polymer ball lens is assembled between two suspended micromachined frames on the Si substrate. In short, it is easy to integrate the ball lens with micromachined structures of different sizes and shapes since the lens is formed from the liquid-phase polymer. Moreover, the fabrication processes are performed at room temperature, and will not damage the existing MEMS structures or ICs (integrated circuits).

The geometry parameters of the micro ball lens and MEMS structures are indicated in figure 4, where D is the diameter of the micro ball lens, h is the thickness of the silicon wafer, d is the diameter of the circular opening on the lens frame, t is the U-shape cross section depth of the lens frame

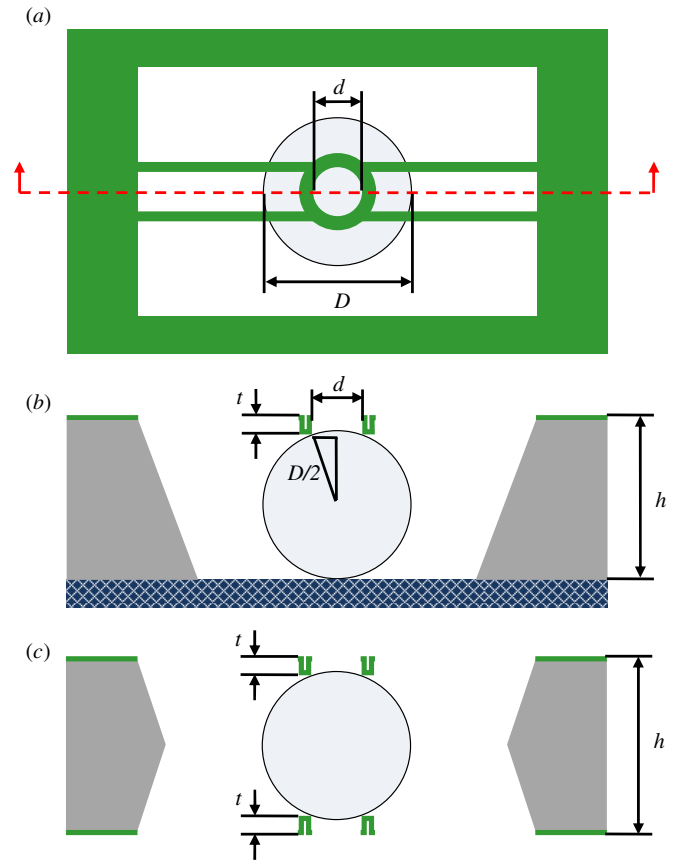


Figure 4. (a) Top view, and (b), (c) cross section views of the micro ball lens and its supporting MEMS structures.

(determined by the trench depth in figure 3(a)). According to the liquid polymer formation technique, the ball lens can be properly fabricated and assembled between the frame and Pyrex glass, despite the lens diameter D being larger than the frame opening d and the frame–glass spacing $h-t$, as indicated in figure 4(b). In the case of figure 4(c), the spacing between the two frames is $h-2t$, which is also smaller than the lens diameter. Note that the frame opening needs to be larger than the outer diameter D_{tip} of the dispensing tip, as indicated in figure 3(d). In application, the presented micro ball lens can be employed to manipulate the light beam incident from both in-plane and out-of-plane directions on the SiOB. For instance, figure 5(a) shows a typical application of the micro ball lens for light condensing in the out-of-plane direction. The direction of light path as indicated in figure 5(a) is suitable for the case of stacking chips. Moreover, figure 5(b) shows the application of the micro ball lens for light collimating in the in-plane direction. The in-plane optical axis depicted in figure 5(b) is beneficial to achieve a SiOB within one chip.

3. Fabrication results

To demonstrate the feasibility of the presented concept, the UV-curable polymer employed in this study was Norland Optical Adhesive 63 (NOA63) with the refractive index of $n = 1.56$, and specific gravity of $s = 1.2$. Glycerol solution diluted with distilled water was selected as the immiscible

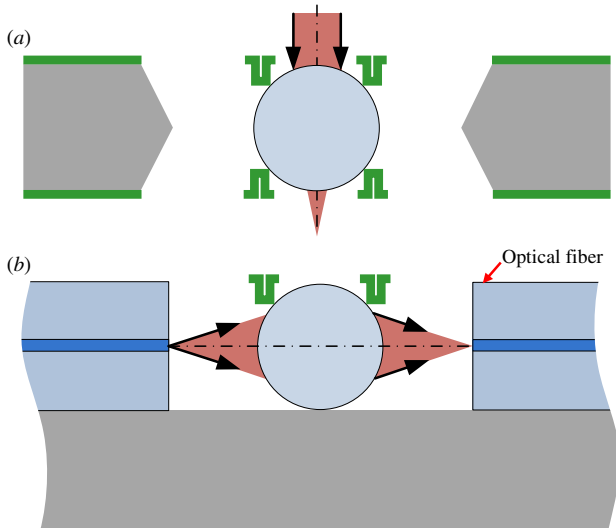


Figure 5. Micro ball lens on SiOB for (a) out-of-plane, and (b) in-plane light condensing/collimating applications.

buffer liquid. The specific gravity of the diluted glycerol solution was near $s = 1.2$. Thus, the immiscible buffer liquid has almost the same density as the dispensed polymer, and the influence of gravitational force was ignored. Firstly, in this study, we dispensed the liquid-phase NOA63 in the diluted glycerol solution to form a discrete ball lens. The photograph in figure 6(a) shows the polymer dispensing process under the buffer liquid. The lens diameter is properly controlled by polymer volume using the commercial pneumatic dispensing system. The dispensing tip indicated in the photograph has an inner diameter of $110\ \mu\text{m}$ and an outer diameter (D_{tip} indicated in figure 3(d)) of $D_{\text{tip}} = 240\ \mu\text{m}$. The liquid polymer lens was then solidified by the UV light curing process. Further cleaning and drying steps were applied to complete the ball lens formation process. The photograph in figure 6(b) shows typical fabricated ball lenses with diameters ranging from 200 to $600\ \mu\text{m}$.

The study further demonstrated the integration of the ball lens with suspended MEMS structures and substrate by means of the processes illustrated in figure 3. The photographs in figures 6(c) and (d) show a typical fabricated polymer ball lens and lens retainer made of thin Si_3N_4 film. The ball lens shown in figure 6(c) was implemented using the process in figures 3(a)–(f). The glassy micro ball lens with a diameter of $D = 525\ \mu\text{m}$ is confined by a transparent glass substrate and thin Si_3N_4 frames. The circular opening of the Si_3N_4 retainer in figures 6(c) and (d) has a diameter of $d = 265\ \mu\text{m}$ to allow the dispensing tip ($D_{\text{tip}} = 240\ \mu\text{m}$) to pass through for polymer dispensing, as in the process shown in figure 3(d). The space between the Si_3N_4 frame and the glass substrate is only $h - t = 476\ \mu\text{m}$ ($< 525\ \mu\text{m}$). It shows the ball lens with diameter D larger than the frame opening d and the gap $h - t$ between the suspended Si_3N_4 retainer and the substrate is successfully assembled and fixed to the chip using the proposed liquid polymer formation technique. Similarly, figure 6(e) shows the ball lens implemented using the process on the right-hand side of figures 3(a)–(f). The micro ball lens

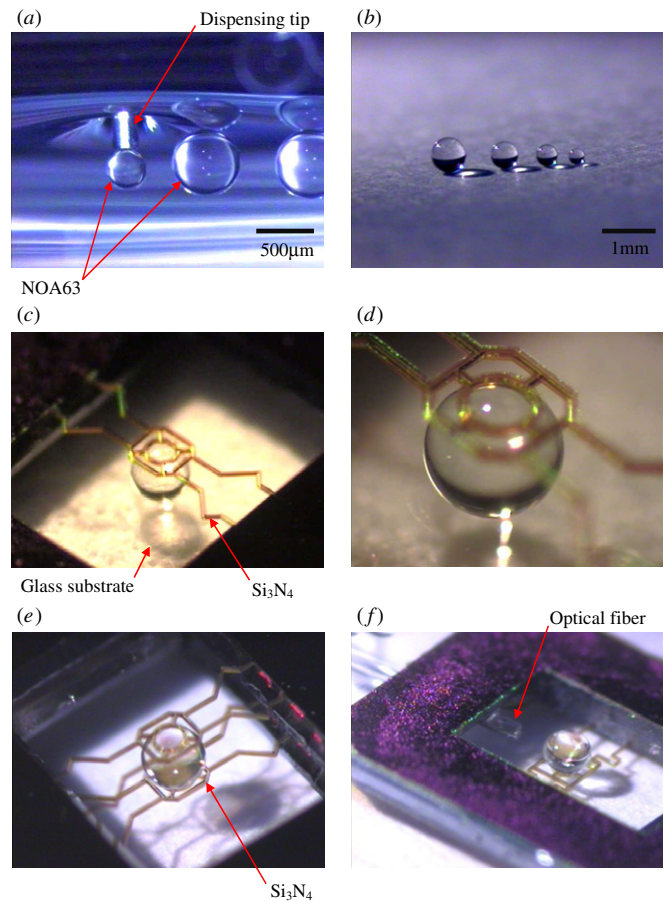


Figure 6. Photographs of the micro ball lens during fabrication and after integration on different SiOBs, (a) dispensing of the polymer under the buffer liquid to form the micro ball lens, (b) typical fabricated micro ball lenses of different diameters, (c) the micro ball lens confined by the micromachined silicon nitride frame and Pyrex glass substrate, (d) zoom-in of the micro ball lens in (c), (e) the micro ball lens supported by two micromachined silicon nitride frames, and (f) the integration of optical fiber with the micro ball lens in (c).

with a diameter of $D = 525\ \mu\text{m}$ is successfully assembled into two suspended Si_3N_4 retainers, although the frame opening is $d = 265\ \mu\text{m}$ and the gap between the suspended Si_3N_4 frames is $h - 2t = 427\ \mu\text{m}$. For both these cases, the light can pass through the ball lens as well as the glass substrate. Thus, the assembled micro ball lenses in figures 6(c)–(e) can be employed to form the out-of-plane SiOB as shown in figure 5(a) using the vertical stacking of chips. On the other hand, the assembled micro ball lenses and optical fiber in figure 6(f) can be employed to form the in-plane SiOB as shown in figure 5(b).

4. Optical measurements

The roundness of the micro ball lens was characterized using the image processing approach with a microscope and commercial software, and the measurement setup is shown in figure 7(a). The tilted rotating stage is employed to characterize the roundness of the ball lens at different viewing angles. As depicted in figure 7(b), the average roundness of

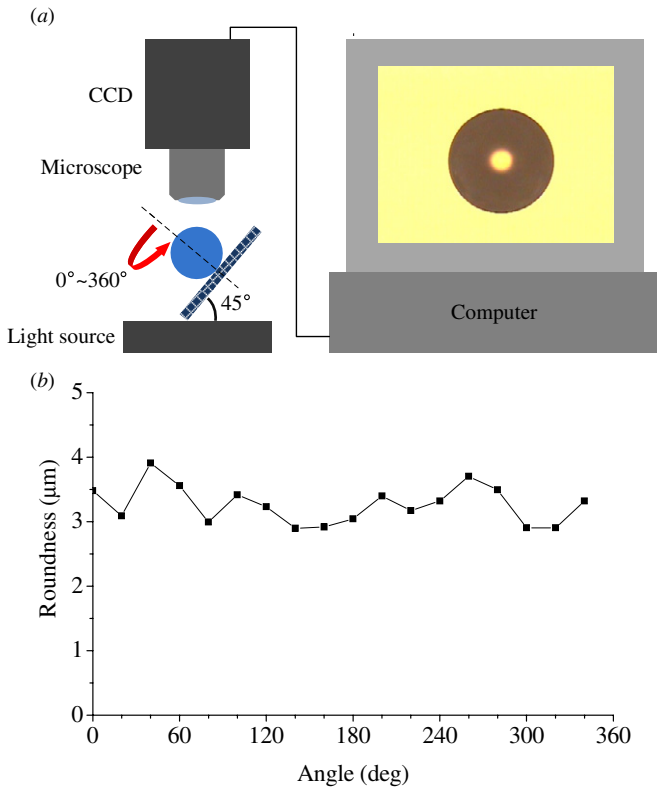


Figure 7. (a) The experimental setup to measure the roundness of the micro ball lens, and (b) the roundness of a 550 μm diameter ball lens observed at different angles.

a 550 μm diameter ball lens observed from different angles is about $3.3 \pm 0.4 \mu\text{m}$ [16]. Moreover, the micro lens has also been evaluated in terms of the radius of curvature (ROC), the RMS surface roughness (Rq), the back focal length (BFL), the effective focal length (EFL) and the optical aberration. In this study, the commercial white light interferometer (WYKO) was employed to characterize the ROC and Rq of the polymer micro ball lens. The typical measured ROC and Rq of the micro lens are 275 μm and 10 nm, respectively.

This study also established the monochromatic Mach-Zehnder interferometer [17–19] as shown in figure 8(a) to characterize the optical aberration of the micro ball lens. As indicated in figure 8(b), the Mach-Zehnder interferometer consists of a laser, an optical fiber, a polarizer, mirrors, beam splitters, and a microscope. The 632.8 nm He–Ne laser is coupled into a single mode fiber (SMF), which acts as a spatial filter [17, 19]. The polarization beam splitter (PBS) is used to split light into a testing beam and a reference beam. The polarizer (POL) is employed to tune the ratio of light intensity between the testing beam and the reference beam to improve the contrast of the interference fringes. The half wave plate (HWP) is used to rotate the polarization of the reference beam by 90°, and after that, the testing beam and the reference beam have the same polarization. In addition, the phase of the reference beam is modulated by the mirror attached to a piezoelectric actuator (PZT). Meanwhile, a long working distance objective (OBJ) with a numerical aperture of $\text{NA} = 0.55$ is exploited to focus the testing beam at the confocal position of the micro ball lens to be characterized.

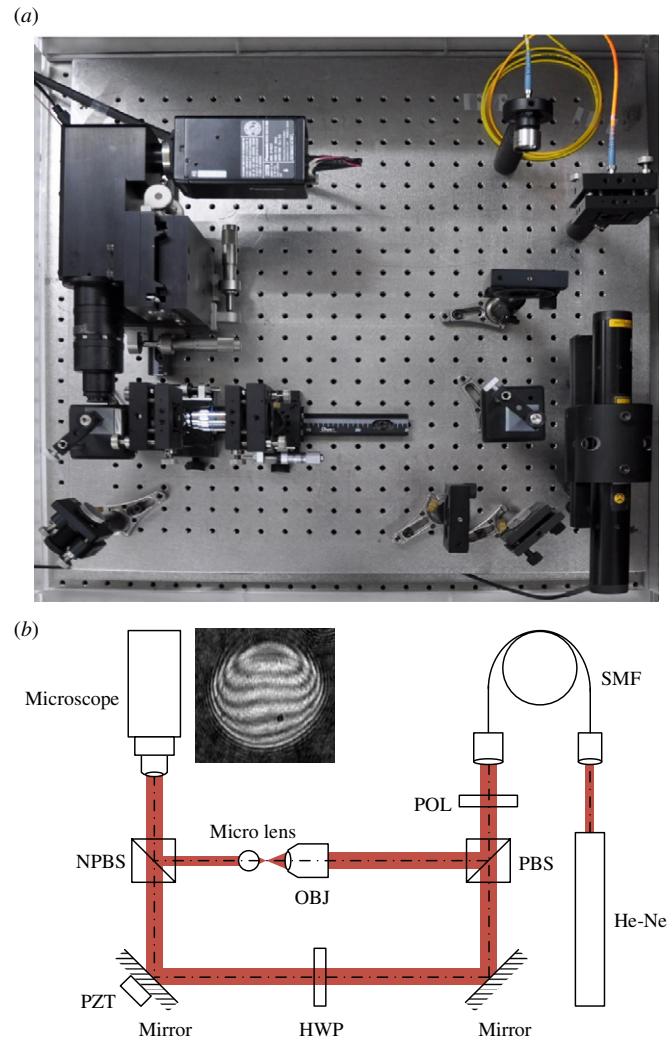


Figure 8. The Mach-Zehnder interferometer setup for wavefront aberration measurement.

Finally, the testing and reference beams are coupled by a non-polarizing beam splitter (NPBS), and then the interferogram is captured by the microscope. The wavefront measured by the Mach-Zehnder interferometer is shown in figure 9 where the peak-to-valley wavefront aberration is 0.3744 waves (237 nm), and the RMS wavefront aberration is 0.0766 waves (48 nm) [18].

Moreover, figure 10 shows the approach to determine the BFL of the micro lens. Firstly, the microscope is focused on the surface of the micro ball lens, as shown in figure 10(a). After that, the micro ball lens is moved until the minimum light spot of the incident He–Ne laser illuminating is observed, as shown in figure 10(b). Thus, the BFL is determined from the moving distance of the micro lens. In this study, the measured BFL was about 99 μm, and the associated EFL was about 351 μm. These measurement results show the micro ball lenses fabricated by the presented insoluble two-phase liquid immersion technology have the same quality as other micro lenses formed on a planar substrate under air ambient conditions [20]. To verify the repeatability of lens formation, in this study, we dispensed and characterized micro ball lenses with diameters ranging from 270 to 500 μm, and 20 samples

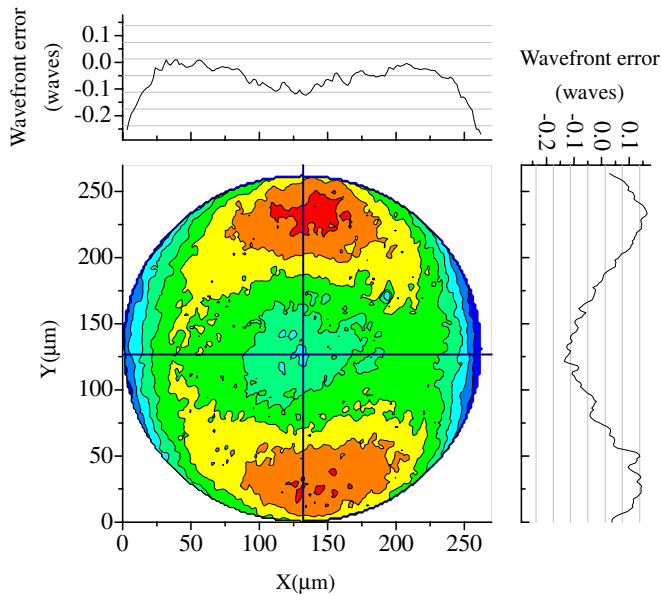


Figure 9. The wavefront error of a 275 μm ROC micro ball lens. The tilt and power of the aberration are removed.

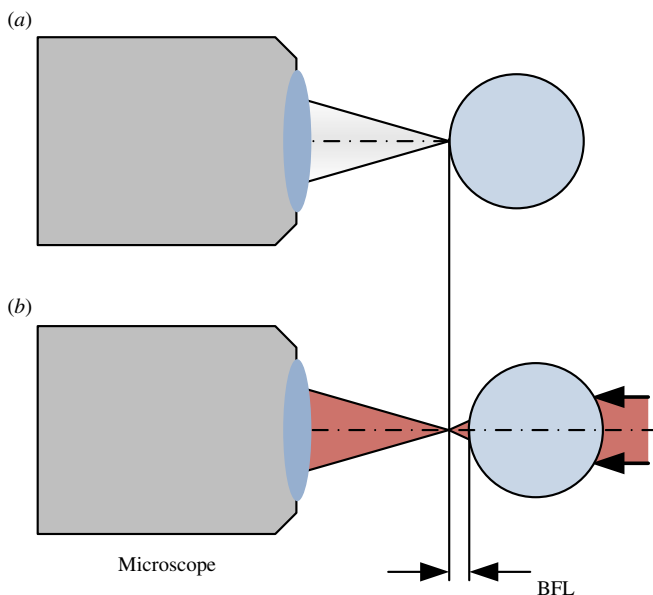


Figure 10. The experimental setup to measure the BFL of micro ball lens.

were measured for each size of lens. The measurements in figure 11 show the distribution of the lens diameter and the BFL for each size of micro ball lens. It can be seen that the presented two-phase liquid micro ball lens formation method has a reasonable repeatability. Moreover, the refractive indices of the NOA63 polymer cured in both air and glycerol were measured. The measurement results, as shown in figure 12, indicate that the refractive index difference is about 0.5%.

5. Conclusions

This study presents a ball lens formation and integration technology utilizing the two-phase liquid approach. The UV-

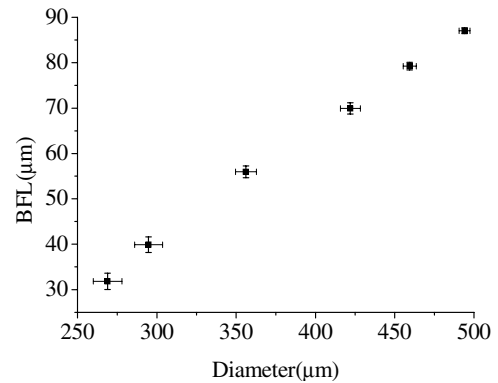


Figure 11. The measured distribution of the lens diameter and the BFL for each size of micro ball lens.

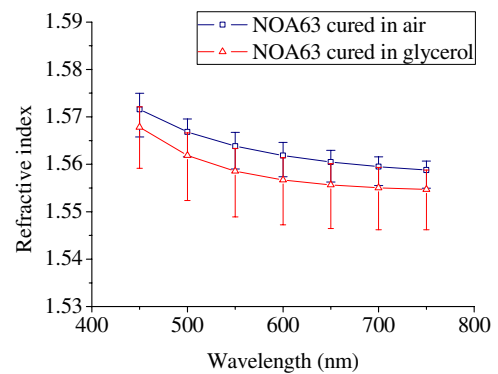


Figure 12. The refractive indices of the NOA63 polymer cured in air and glycerol, respectively.

curable polymer is dispensed into a buffer liquid to form the ball lens. Thus, the buffer liquid can provide a gravity-free condition to enable the ball lens with a highly symmetric shape. The diameter of the ball lens is controlled by the volume of the dispensed polymer. In application, the formation of the NOA63 polymer ball lens in glycerol buffer liquid is demonstrated. The typical ball lens diameter ranges from 200 to 600 μm , and its surface roughness measured by an optical interferometer is about 10 nm. The average roundness of a 550 μm diameter ball lens measured from different angles is $3.3 \pm 0.4 \mu\text{m}$. According to the measurement results of a Mach-Zehnder interferometer, the peak-to-valley and RMS wavefront errors of a 550 μm diameter ball lens are 237 nm and 48 nm, respectively. The measured BFL is about 99 μm , and the associated EFL is about 351 μm . The presented approach can be further employed to implement polymer ball lenses of different materials. Moreover, the integration of the micro ball lens with a suspended micromachined thin Si_3N_4 structure is also demonstrated.

Acknowledgments

This work was supported partially by the Ministry of Economic Affairs, Taiwan, under contract number 97-EC-17-A-07-S1-011, and by the National Science Council, Taiwan, under contract number NSC-96-2628-E-007-008-MY3.

References

- [1] Walker J A 2000 The future of MEMS in telecommunications networks *J. Micromech. Microeng.* **10** R1–7
- [2] Schwarz R A, Arifler D, Chang S K, Pavlova I, Hussain I A, Mack V, Knight B, Richards-Kortum R and Gillenwater A M 2005 Ball lens coupled fiber-optic probe for depth-resolved spectroscopy of epithelial tissue *Opt. Lett.* **30** 1159–61
- [3] Jiang W, Sun Y, Chen R T, Guo B, Horwitz J and Morey W 2002 Ball-lens based optical add-drop multiplexers: design and implementation *IEEE Photonics Technol. Lett.* **14** 825–7
- [4] Sasaki M, Nakai F, Hane K, Yokomizo K and Hori K 2006 Absolute micro-encoder using image obtained by ball lens assembled inside wafer *J. Opt. A: Pure Appl. Opt.* **8** S391–7
- [5] Huby N, Pluchon D, Coulon N, Belloul M, Moreac A, Gaviot E, Panizza P and Beche B 2010 Design of organic 3D microresonators with microfluidics coupled to thin-film processes for photonic applications *Opt. Commun.* **283** 2451–6
- [6] Kim Y S, Kim J, Choe J S, Rob Y G, Jeon H and Woo J C 2000 Semiconductor microlenses fabricated by one-step wet etching *IEEE Photonics Technol. Lett.* **12** 507–9
- [7] O'Neill F T and Sheridan J T 2002 Photoresist reflow method of microlens production: part I. Background and experiments *Optik—Int. J. Light Electron Opt.* **113** 391–404
- [8] Lee S-K, Lee K-C and Lee S S 2002 A simple method for microlens fabrication by the modified LIGA process *J. Micromech. Microeng.* **12** 334–40
- [9] Audran S, Faure B, Mortini B, Regolini J, Schlatter G and Hadziioannou G 2006 Study of mechanisms involved in photoresist microlens formation *Microelectron. Eng.* **83** 1087–90
- [10] Cox W R, Chen T, Hayes D J and Grove M E 2001 Microjet printing of micro-optical interconnects for telecom devices *Proc. SPIE* **4292** 208
- [11] Shen S C and Huang J C 2009 Rapid fabrication of a micro-ball lens array by extrusion for optical fiber applications *Opt. Express* **17** 13122–7
- [12] Hsieh J, Hsiao S-Y, Lai C F and Fang W 2007 Integration of a UV curable polymer lens and MUMPs structures on a SOI optical bench *J. Micromech. Microeng.* **17** 1703–9
- [13] Lee C-C, Hsiao S-Y and Fang W 2009 Formation and Integration of a ball lens utilizing two phase liquid technology *Proc. IEEE MEMS (Sorrento, Italy)* pp 172–5
- [14] Han M-G, Park Y-J, Kim S-H, Yoo B-S and Park H-H 2004 Thermal and chemical stability of reflowed-photoresist microlenses *J. Micromech. Microeng.* **14** 398–402
- [15] Lin H-Y and Fang W 2000 Rib-reinforced micromachined beam and its applications *J. Micromech. Microeng.* **10** 93–9
- [16] Smith G T 2002 *Industrial Metrology: Surfaces and Roundness* (London: Springer)
- [17] Sickinger H, Schwider J and Manzke B 1999 Fiber based Mach-Zehnder interferometer for measuring wave aberrations of microlenses *Optik* **110** 239–43
- [18] Reichelt S, Bieber A, Aatz B and Zappe H 2005 Micro-optics metrology using advanced interferometry *Proc. SPIE* **5856** pp 437–46
- [19] Gomez V, Ghim T-S, Ottevaere H, Gardner N, Bergner B, Medicus K, Davies A and Thienpont H 2009 Micro-optic reflection and transmission interferometer for complete microlens characterization *Meas. Sci. Technol.* **20** 025901
- [20] Ottevaere H, Cox R, Herzig H P, Miyashita T, Naessens K, Taghizadeh M, Volkel R, Woo H J and Thienpont H 2006 Comparing glass and plastic refractive microlenses fabricated with different technologies *J. Opt. A: Pure Appl. Opt.* **8** S407–29